

# **RERTR 2022 – 42<sup>ND</sup> INTERNATIONAL MEETING ON REDUCED ENRICHMENT FOR RESEARCH AND TEST REACTORS**

**OCTOBER 3-5, 2022**

**VIENNA INTERNATIONAL CENTRE**

**VIENNA, AUSTRIA**

## **About the limits of optical microscopy for research reactor fuel cladding depth measurement**

N. Hibert <sup>1</sup>, O. Tougait <sup>1</sup>,

<sup>1</sup> Unité de Catalyse et Chimie du Solide, Université de Lille, Cité Scientifique, F-59650  
Villeneuve d'Ascq, - France

A. Megzari <sup>2,3</sup>, G. Despaux <sup>2</sup>, E. Le Clézio <sup>2</sup>

<sup>2</sup> IES, Univ Montpellier, CNRS, Montpellier, - France

B. Stepnik<sup>3</sup>

<sup>3</sup> Framatome, CERCA, SPL, ZI Les Bérauds, 54 avenue de la déportation, BP 114, F-  
26104 Romans-sur-Isère - France

### **ABSTRACT**

The Al-based cladding is the only barrier to radionuclide release for pool research reactors, so its integrity must be scrupulously preserved until the core assemblies are reprocessed. At each production stage stringent controls are carried out, such as dimensional examinations, visual inspections as well as a final blister test. In addition to these non-destructive tests, randomly selected fuel plates are also sampled for direct measurement of the cladding thickness as quality control measures. This additional control consists in taking cuts from specific areas of the fuel-plate which, once polished, are subject to a metrological measurement. This destructive examination, which is time and cost-consuming, would need to be replaced especially since optical measurements also have their own limits. In this work, we have attempted to stretch the limits of optical measurements to find the best compromise between high level of accuracy and effectiveness.

### **1 Introduction**

In the framework of securing nuclear fuel supply for European research reactor, low enriched uranium “LEU” fuels are being considered as promising candidates [1–4]. Dispersed nuclear fuels for European research reactor are typical fuel-plates, comprising as fissile material, UMo [1] or U<sub>3</sub>Si<sub>2</sub> particles [2], dispersed in an Al matrix, and clad with an Al-based alloy.

The Al-cladding represents the first barrier of containment for fission products. In the pool, the cladding must meet the requirements of limited corrosion and preservation of mechanical properties, thus ensuring the safety of the reactor. The dispersed fuel-plates must respect a minimum value of the cladding thickness, which has to be controlled at the fabrication process. Thus, determining the cladding depth is paramount for the manufactured nuclear fuel as quality control measures.

The cladding depth measurement relies on metrological measurements on cladding cross-section using optical microscopy, after suitable surface preparation [1]. This method is destructive, time-consuming and operator-biased. Indeed, both the polishing and image acquisition procedures need to be carefully performed in order to properly evaluate the length measurements.

The surface preparation comprises grinding followed by polishing. Similarly, the image acquisition requires suitable lighting, the appropriated magnification and the measurement demands adjusted step-size and the baseline as well as a calibration.

All these steps cannot be automated in a single quality control process, but require careful attention since they are prone to random and operator errors, especially when hundreds of measurements per sample are involved. In this study, we tried to reach the precision and efficiency limits of the optical image method of cladding depth-measurement.

## 2 Experimental

### 2.1 Material

The fuel-plate fabrication were performed at CERCA/Framatome, following a 4-step process: Cold pressing of the fissile material and Al powder mixture in a compact 2) Embedding in an Al cladding frame, 3) Hot-rolling for several reduction passes, 4) Blistering test for ensuring the adherence between the multiple layers and absence of blisters [1,5,6].

The examined fuel plates comprise  $U_3Si_2$  grinded particles or UMo atomized kernels as fissile material corresponds. The cladding is AG3NE. The hot-rolled plates were examined at various steps, from 2.4 to 1.2mm. A summary of the sample features is given in Table 1. Several cuts of  $9 \times 28 \text{ mm}^2$  were punched at selected locations of the fuel plates.

Thickness	Meat (dispersed in Al matrix)	Meat physical form	Type of cladding	Number of studied samples
1,2 mm	$U_3Si_2$	Grinded particles	AG3NE alloy	8
2.4 mm	U-7%wt.Mo	Atomized kernels	AG3NE alloy	2

Table 1 \_ Description of the fuel plates used in this study

Before being cut, 6 Vickers indentations were made on one face of the sample in order to pin point the cross-section and the sample orientation (fig.1). The indentation, applied with a 3 kg weight, corresponds to a squared footprint with  $230 \mu\text{m}$  sides and  $330 \mu\text{m}$  diagonals. The cladding deep measurements have been performed between the two indentations 20 mm apart for each other, as illustrated in fig.1, A) by the blue diamond symbols. The four remaining indentations (green diamond symbols) were used for the sample orientation and to serve as reference points to assess the observed cross-section location once the grinding and polishing steps over.

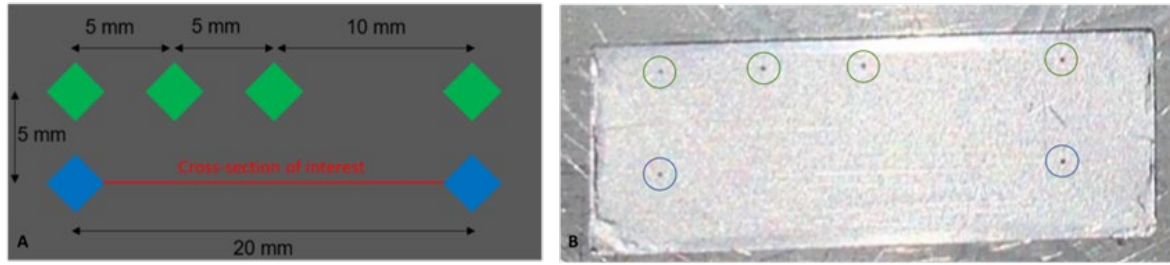


Figure 1 \_ A) Sample representation with indentations highlighted (warning: indentation not to scale) and with the measurement line as the solid red line, B) Sample optical image with 6 indentations circled in green and blue

## 2.2 Methods

### 2.2.1 Mechanical grinding and polishing

The polishing procedure had two purposes, grinding up to the measurement line and obtaining a defect-free surface for the metrology.

The objective of the grinding was to reveal the measurement line which goes through the center of the diamond indentation points. The grinding and polishing steps were performed with a STRUERS Tegramin 30 polishing equipment using a home-made vice sample-holder carrying only one sample each time. This individual preparation is due to a measurement line located at a different height. The applied pressure was transmitted manually. The amount of removed material was regularly checked.

The grinding was performed by using a judicious set of polishing papers. To remove most of the material, abrasive polishing papers from 30 $\mu$ m up to 15 $\mu$ m were used during several minutes (1-5min). When less than 1mm was needed to be removed from the material, 10 $\mu$ m paper was used. To obtain a surface with the less damage as possible, the polishing was carried out with a set of polishing cloths associated with diamond suspensions, from 6 $\mu$ m down to 1 $\mu$ m during 5-10min.

In order to mitigate edge-effect defects, which hindered accurate detection of the sample edge, sacrificial plates were introduced during both grinding and polishing processes. The sample was sandwiched between two Al plates during grinding (fig.2, A). A transparent PVC plate was put next to the indented face of the sample during polishing (fig.2, B) to prevent edge-effect defects but also to be able to visualize the material removing progress during the final step of grinding.

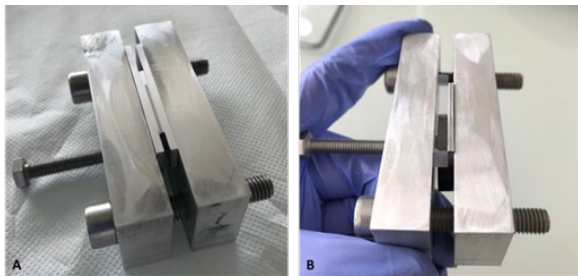


Figure 2 \_ Home-made vice as sample holder, plate sample being sandwiched between A) Al sacrificial plates, B) PVC sacrificial plates next to the indented face of the sample

### 2.2.2 Collecting optical images

Keyence latest VHX 7000 digital microscope was used to collect the optical images. The Keyence image treatment built-in software was used to carry out the length measurements. Upon starting, the microscope follows a calibration procedure ensuring a reliable image acquiring process for all the available lenses. The resolution ( $\mu$ m/pixel) depends on the lens used.

In order to determine the observed cross-section location resulting from the grinding and polishing steps, two images of the indented sample face were collected. The two pictures were recorded at the two residual indentation locations, 20 mm apart. Those pictures (2880x2160 pixels, with 2,6 $\mu\text{m}$ /pixel) were collected using a X40 lens with a circular lightning.

Reconstructed cross-section images were collected using the X300 lens with a mixed lightning (90% circular and 10% coaxial). In order to visualize the entirety of the 20 mm cross-section, 3 reconstructed images were collected and combined. The X300 lens was found to be the best compromise between time, resolution and file size (11800x1083 pixels, with 0,65 $\mu\text{m}$ /pixel).

Some overlapping was necessary to merge the 3 reconstructed cross-section images together. Careful attention was paid to guarantee the cross-section horizontality along the 20 mm and the X-Y initialization of the microscope observation deck.

### 2.2.3 Length measurements

All length measurements were performed on Keyence image treatment built-in software. Two kinds of optical length measurements were performed.

Firstly, on the indented face images, the length between the residual indentations of interest (those 20mm apart) and their above indentations was measured (fig.3, A and B). Those measurements allowed an accurate determination of the obtained cross-section location resulting from the grinding and polishing steps.

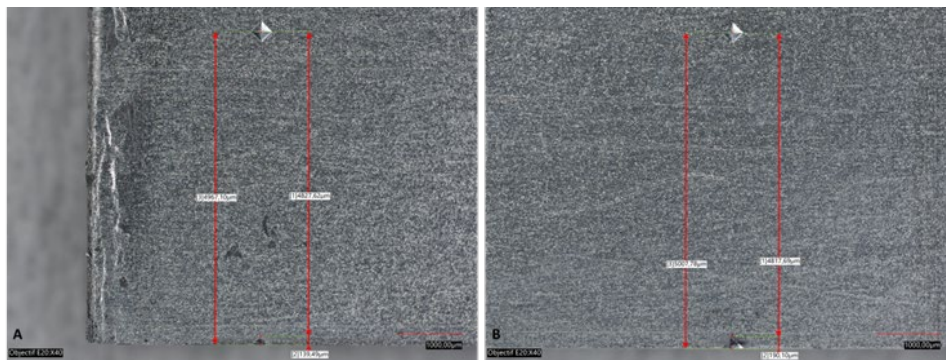


Figure 3 \_ Determiration the obtained cross-section location after grinding and polishing steps, A) Right end side indentation and B) Left end side indentation

Secondly, on the 3 reconstructed cross-section images, individual cladding depth measurements were carried out with a 50  $\mu\text{m}$  step-size. The “cladding depth” corresponds to the distance between the sample border and the cladding-meat interface (fig.4).

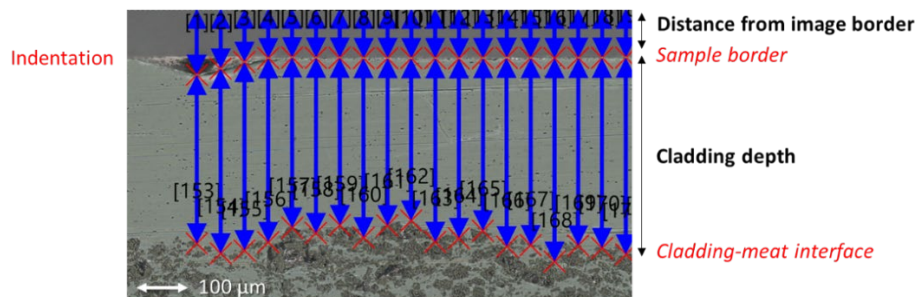


Figure 4\_ Reconstructed cross-section image with optical measurements, distance from the image border and the cladding depth

In total, 400 individual measurements were performed along the 20mm length. All measurements were done manually by applying a mesh scale with a size-step of 50 $\mu$ m. The 400 measurements were concatenated as a depth-line, to be subsequently superposed on the merged whole cross-section image.

In order to match the sample border profile along the 20mm cross-section, the distance between the sample border and the image border was also collected along a perpendicular line according to the mesh scale (fig.4). Furthermore, a sample with UMo kernel was studied additionally with a 5 $\mu$ m step-size over a 10mm length.

### 3 Results

#### 3.1 Optical image procedure optimization

The first preparation tests were carried out without sacrificial plates (Al or PVC) and led to unsatisfactory results, as shown in the fig.5 A) and B). A strong impact of mechanical-induced edge-effect phenomena on the sample border was observed. On fig.5 A), the circular lightening led to a sub-optimal meat-cladding interface visualization and a loose sample border detection. On fig.5 B), the coaxial lightening was useless to ascertain the sample edge (highlighted in red) which cannot be distinguished due to edge-effect induced “shadowing”.

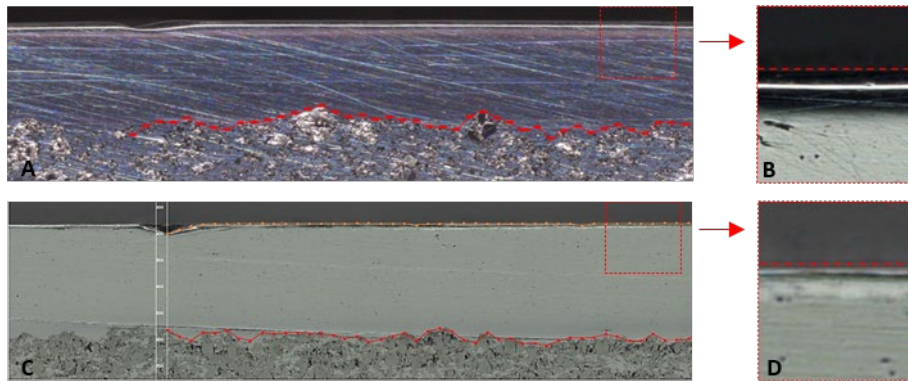


Figure 5 \_ Optical images of cross-sections with different level of edge-effect impact, A) Sample with strong impact from edge-effect, B) Zoom on the sample border with high edge-effect, C) Sample with minimal impact from edge-effect and D) Zoom on the sample border with low edge-effect

In order to mitigate the edge-effect impact induced during the polishing steps, sacrificial plates were introduced for the subsequent preparation tests. Results obtained with sacrificial plates were more satisfying, as illustrated in the fig.5 C) and D). Both images were recorded with a mix lightening (90% circular and 10% coaxial), enabling an accurate meat-cladding interface visualization and precise sample edge detection. On the fig.5 D), the red-highlighted borderline correctly matches the visible edge of the sample.

#### 3.2 Al-cladding depth measurements

In total, 8 U<sub>3</sub>Si<sub>2</sub> and 2 UMo samples were studied with a 50 $\mu$ m step-size. Fig.6 displays the sample borderlines (orange) and the cladding depth-lines (pink) resulting from the concatenation of the 400 optical measurements of a U<sub>3</sub>Si<sub>2</sub> sample (A) and UMo sample (B). Only small sections of reconstructed cross-section images are showed as they are too large to be displayed in their entirety.

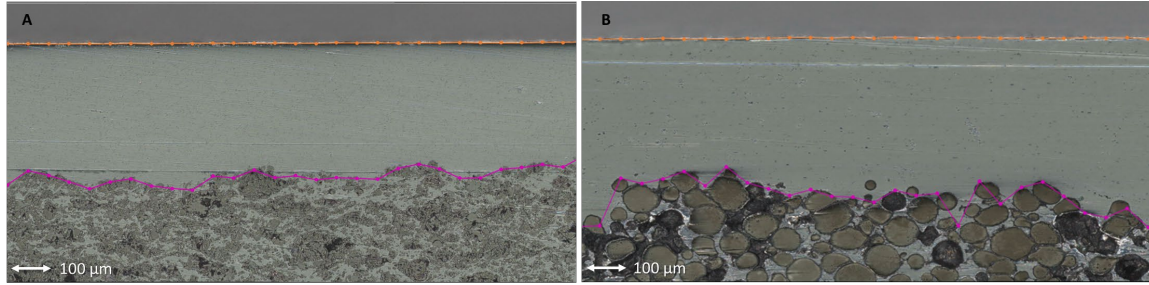


Figure 6 \_ Superposition of the borderline (orange) and the depth-line (pink), A) U3Si2 sample and B) UMo sample

Due to the 50 $\mu$ m step-size, some mismatch is occurring between the cladding depth-line and the actual cladding-meat interface. This issue underlines that optical microscopy is a discrete method of cladding depth measurement. The smaller the step-size, the better the matching will be.

As it was found that UMo samples were more prone to mismatch, a follow-up study was made with a step-size of 5 $\mu$ m. The decrease of the step-size gave a more trustworthy detection of the cladding-meat interface, as it is demonstrated on Fig.7.

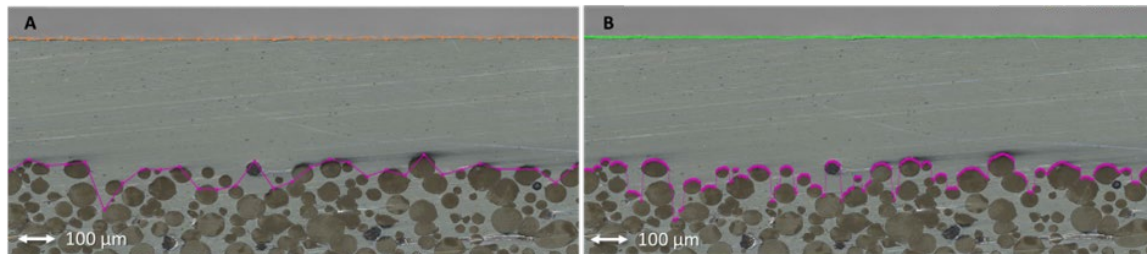


Figure 7 \_ Superposition of the borderline (orange or green) and depth-line (pink) for a UMo sample at the same location on the cross-section with different step-size, A) 50  $\mu$ m and B) 5  $\mu$ m

However, having a step-size of 5 $\mu$ m increased greatly the completion time of all the measurements. Thus, it was found that a step-size of 50 $\mu$ m was the most suitable to reach the requirements of efficiency and accuracy for both types of samples.

In order to evaluate the uncertainties attached to optical microscopy, several repeatability tests were performed about the cross-sections, cladding depth and step-size measurements. From our experimental results, the uncertainties on the cross-section location and the cladding depth are less than 1  $\mu$ m while the step-size is respected to 10nm (table.2).

Parameter studied	Type of measurement	Number of measurements	Standard deviation ( $\mu$ m)	Uncertainties $k = 2$ ( $\mu$ m) [7]
<b>Cross-section location</b>	Distance between one indentation of interest and its above indentation	10	0,59	0,37
<b>Cladding depth</b>	Distance between sample border and cladding-meat interface on a perpendicular line	200	1,00	0,77
<b>Step-size</b>	Distance applied by the mesh scale provided by the built-in software	4000	0,04	0,01

Table 2 \_ Uncertainties attached to optical microscopy method obtained from this study, associated with the type of measurement used by parameter studied

The uncertainties are close to the ones obtained by previous Framatome experimental results (about 1  $\mu\text{m}$ ), using a different optical microscope and imaging software.

#### 4 Conclusion

In this study, in-house designed experimental methods were introduced, based on previous Framatome procedures for the fabrication control. It is demonstrated that a careful grinding-polishing process allows the removal of the desired amount of material, to obtain a scratch-free cross-section surface. Such surface preparation allows acquisition of high-quality images needed to determine cladding depth with sufficient accuracy and good efficiency.

From the optical measurements, this study produced 10 trustworthy databases of cladding-depth for  $\text{U}_3\text{Si}_2$  and UMo dispersed fuel cuts. Also, it was found that a smaller step-size allows a more trustworthy detection of the meat-cladding interface but also make the measurements much more time-consuming.

Finally, uncertainties were calculated to be less than 1  $\mu\text{m}$  for cladding depth measurements, which is lower than the value obtained by previous experimental results from Framatome.

#### 5 Acknowledgement

This work was funded by EURATOM research and training program 2014-2018 under grant agreement LEU FOREVER n°754378. The authors would like to thank Framatome for producing the nuclear fuel plate samples and for funding this study. Chevreul Institute (FR 2638), Ministère de l'Enseignement Supérieur, de la Recherche et de l'Innovation, Hauts-de-France Region, the joint intergated laboratory PUMA (Framatome-CNRS-University of Lille, Centrale Lille Institute) is acknowledged for supporting this work.

#### 6 References

- [1] B. Stepnik, M. Grasse, C. Rontar, D. Geslin, Y. Guinard, S. Van den Berghe, A. Leenaers, H. Breitzkreutz, W. Petry, H. Palancher, E. Hervieu, Y. Calzavara, H. Guyon, Manufacturing of the SEMPER FIDELIS UMo irradiation experiment (2018 RRFM Conference) Proceedings of the 22sd International Meeting on Research Reactor Fuel Management, Munich, Germany, (2018).
- [2] D.D. Keiser, D.M. Wachs, A.B. Robinson, W.J. Williams, M. Lillo, N.E. Woolstenhulme, G.A. Moore, J.-F. Jue, G.L. Hofman, The use of  $\text{U}_3\text{Si}_2/\text{Al}$  dispersion fuel for high power research reactors, *J. Nucl. Mater.* 528 (2020) 151820. <https://doi.org/10.1016/j.jnucmat.2019.151820>.
- [3] S. Van den Berghe, P. Lemoine, Review of 15 years of high-density lowenriched UMo dispersion fuel development for research reactors in Europe, *Nucl. Eng. Technol.* 46 (2014) 125–146. <https://doi.org/10.5516/NET.07.2014.703>.
- [4] S. Valance, H. Breitzkreutz, Y. Calzavara, M. Hrehor, F. Huet, J. Jaroszewicz, H. Palancher, B. Stepnik, S. Van Den Berghe, The H2020 european project fuel for research reactors LEU – forever : leu fuels for medium and high power research reactors in Europe, International Topical Meeting on Research Reactor Fuel Management, Mar 2018, Munich, Germany, (2019). <https://hal-cea.archives-ouvertes.fr/cea-02339322>.
- [5] J.P. Durand, B. Duban, Y. Lavastre, S. De Perthuis, CERCA's 25 Years Experience in  $\text{U}_3\text{Si}_2$  Fuel Manufacturing \_ 2003 International RERTR Meeting, Int. Meet. Reduc. Enrich. Res. Test React. (2003). <https://www.osti.gov/etdeweb/servlets/purl/20468650>.
- [6] C. Jarousse, Y. Lavastre, M. Grasse, CERCA'S EXPERIENCE IN UMO FUEL

- MANUFACTURING \_ 2003 International RERTR Meeting, Int. Meet. Reduc. Enrich. Res. Test React. (2003). <https://www.osti.gov/etdeweb/servlets/purl/20494066>.
- [7] Joint Committee for Guides in Metrology, Évaluation Des Données De Mesure — Guide Pour L'expression De L'incertitude De Mesure (JCGM/WG 1), JCGM 1002008. (2008). [https://www.bipm.org/utis/common/documents/jcgm/JCGM\\_100\\_2008\\_F.pdf](https://www.bipm.org/utis/common/documents/jcgm/JCGM_100_2008_F.pdf).